FREE RADIATION AND MASS TRANSFER EFFECTS ON MHD CONVECTION FLOW ALONG A MOVING VERTICAL POROUS PLATE WITH SUCTION AND CHEMICAL REACTION IN PRESENCE OF SORET AND DUFOUR EFFECTS

E.HEMALATHA[1], A.NEERAJA[2 *], R.L.V.RENUKA DEVI[3]

2 Department of Mathematics, Aditya College of Engineering, Surampalem, East Godavari Dt-533437., Andhra Pradesh,India.

1,3 Department of Mathematics, Sri Venkateswara University, Tirupati-517502, Andhra Pradesh. India.

**Corresponding author: A.Neeraja, E-mail addresses: dr.neeraja27@gmail.com*

ABSTRACT

The paper deals with the study of the radiation and chemical reaction on MHD boundary layer flow of a moving vertical porous plate embedded in a porous medium by taking Soret and Dufour effects and heat source into account. The equations governing the flow are coupled and solved numerically using Runge - Kutta fourth order method along with Newton Raphson shooting technique. The influence of various governing parameters on the velocity, temperature, concentration, skin-friction coefficient, Nusselt number and Sherwood number and discussed in detail. The results are compared with those available in literature obtained through analytical procedures and seen to be in good agreement.

KEY WORDS：Radiation, Mass transfer,Chemical reaction, Soret, Dufour.

1. INTRODUCTION

Boundary layer flows past a vertical surface are common in engineering problems in industry. Some practical areas of application include metal and polymer extrusion processes, wire drawing, chemical coating of flat plates and hot rolling. Many chemical engineering processes like metallurgical and polymer extrusion involve cooling of molten liquid. Soundalgekar [1] studied the effects of convection on the Stokes problem past an infinite vertical plate. Later Soundalgekar [2] extended his own problem to mass transfer case. Bejan and Khair [3] studied the effects of heat and mass transfer on natural convection flow in a porous medium. Cortell [4] studied the radiation effects with heat transfer on power-law fluid past an infinite porous plate in the presence of suction and viscous dissipation.Kafoussias and Williams [5] presented the Soret and Dufuor effects on a mixed convective steady laminar boundary layer flow past a vertical flat plate. Ibrahim et al. [6] studied the effects of chemical reaction on hydromagnetic flow along a continuously moving permeable surface in the presence of heat source with time dependent suction and radiation absorption. Kandaswamy et al. Ibrahim and Makinde [7] studied the effect of chemical reaction on MHD boundary layer flow of heat and mass transfer along a moving vertical plate with suction. Srinivasa Rao et al [8] presented the Soret and Dufour effects on magnetohydrodynamic boundary layer flow past a moving vertical porous plate in the presence of suction.However, no attempt has been made to analyze effects of radiation and chemical reaction on MHD boundary layer flow of a moving vertical porous plate embedded in a porous medium by taking Soret and Dufour effects and heat source into account. Hence an attempt is made to study this problem.

2. MATHEMATICAL ANALYSIS

Two-dimensional steady boundary layer flow of a viscous incompressible electrically conducting, radiating and chemically reacting fluid past a linearly started porous semi-infinite vertical plate embedded in a porous medium with Soret and Dufour effects in presence of chemical reaction is considered. Under these assumptions along with usual Boussinesq and boundary layer approximations the system of equations, which models the flow is given by

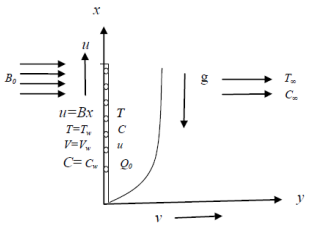

Fig. 1: Schematic diagram of the physical model

Continuity equation

$$\frac{\partial u}{\partial x}+\frac{\partial v}{\partial y}=0 \qquad (1)$$

Momentum equation

$$u\frac{\partial u}{\partial x}+v\frac{\partial u}{\partial y}=\upsilon\frac{\partial^2 u}{\partial y^2}+g\beta\left(T-T_\infty\right)+g\beta^*\left(C-C_\infty\right)-\frac{\sigma B_0^2}{\rho}-\frac{\upsilon}{K'}u \qquad (2)$$

Energy equation

$$u\frac{\partial T}{\partial x}+v\frac{\partial T}{\partial y}=\alpha\frac{\partial^2 T}{\partial y^2}+\frac{Q_0}{\rho C_p}(T-T_\infty)\frac{D_m K_T}{C_s C_p}\frac{\partial^2 C}{\partial y^2}-\frac{1}{\rho C_p}\frac{\partial q_r}{\partial y} \qquad (3)$$

Species equation

$$u\frac{\partial C}{\partial x}+v\frac{\partial C}{\partial y}=D_m\frac{\partial^2 C}{\partial y^2}+\frac{D_m K_T}{T_m}\frac{\partial^2 T}{\partial y^2}-Kr'C \qquad (4)$$

where u and v are the velocity components in x and y directions, υ is the kinematics viscosity, g is the acceleration due to gravity, β is the coefficient of thermal expansion, β^* is the coefficient of thermal expansion, respectively, T is the temperature of the fluid, C is the species concentration in the boundary layer, T_∞ is the temperature for away from the plate, C_∞ Species concentration of the ambient fluid, σ is the electric conductivity of the fluid, B_0 is the uniform magnetic field, ρ is the density, K' is the permeability, α is the thermal diffusivity, Q_0 - the heat generation coefficient, C_p - the specific heat at constant pressure, D_m is the mass diffusivity, K_T is the thermal diffusion ratio, C_s is the concentration susceptibility, C_p is the specific heat at constant pressure, q_r is the radiative heat flux, T_m is the mean fluid temperature and Kr' is the chemical reaction rate on the species concentration.

The boundary conditions for the velocity, temperature and concentration fields are

$u = B\,x$, $v = V$, $T = Tw = T_\infty + ax$, $C = C_w = C_\infty + bx$ at $y=0$

$u \to 0$, $T \to T_\infty$, $C \to C_\infty$ as $y \to \infty$ (5)

where B is a constant, a and b denote the stratification rate of the gradient of ambient temperature and concentration, V is the suction velocity at the plate.

By using the Rosseland approximation (Brewster[9]), the heat flux q_r is given by

$$q_r = \frac{4\sigma^*}{3k^*}\frac{\partial T^4}{\partial y} \tag{6}$$

$$T^4 = 4T_\infty^3 T - 3T_\infty^4 \tag{7}$$

In view of the equations (6) and (7), the equation (3) reduces to

$$u\frac{\partial T}{\partial x} + v\frac{\partial T}{\partial y} = \alpha\frac{\partial^2 T}{\partial y^2} + \frac{Q_0}{\rho C_p}(T - T_\infty) + \frac{D_m K_T}{C_s C_p}\frac{\partial^2 C}{\partial y^2} + \frac{16\sigma^* T_\infty^3}{3k^*\rho c_p}\frac{\partial^2 T}{\partial y^2} \tag{8}$$

The continuity equation (1) is satisfied by the Cauchy Riemann equations

$$u = \frac{\partial \psi}{\partial y} \text{ and } v = -\frac{\partial \psi}{\partial x} \tag{9}$$

where $\psi(x,y)$ is the stream function.

In order to write the governing equations and the boundary conditions in the dimensionless form, the following similarity variables and dimensionless quantities are introduced.

$$\eta = \sqrt{\frac{B}{\upsilon}}y, \quad f(\eta) = \frac{\psi}{x\sqrt{B\upsilon}}, \quad \theta(\eta) = \frac{T - T_\infty}{T_f - T_\infty}, \quad \phi(\eta) = \frac{C - C_\infty}{C_w - C_\infty},$$

$$f_w = \frac{V}{\sqrt{B\upsilon}}, \quad Gc = \frac{g\beta^*(C_w - C_\infty)}{xB^2}, \; M = \frac{\sigma B_0^2}{\rho B}, \; Du = \frac{D_m K_T}{C_s C_p \upsilon}\frac{(C_w - C_\infty)}{(T_w - T_\infty)},$$

$$S = \frac{Q_0}{B\rho C_p}, \; Sr = \frac{D_m K_T (T_w - T_\infty)}{T_m \upsilon (C_w - C_\infty)}, \; \Pr = \frac{\upsilon}{\alpha}, \; Sc = \frac{\upsilon}{D}, \; Kr = \frac{Kr'}{B}, \tag{10}$$

$$K = \frac{\upsilon}{K'B}, \; Nc = \frac{C_\infty}{C_w - C_\infty}, \; R = \frac{4\sigma^* T_\infty^3}{3k^* k}$$

In the view of the above similarity transformations, the equations (2), (3) and (6) reduce to

$$f''' + ff'' - (f')^2 + Gr\theta + Gc\phi - (M + K)f' = 0 \tag{11}$$

$$(4R+1)\theta'' + \Pr(f\theta' - f'\theta) + Du\Pr\varphi'' + \Pr S\theta = 0, \tag{12}$$

$$\varphi'' + Sc(f\varphi' - f'\varphi) + ScSr\theta'' - ScKr(\varphi + Nc) = 0 \tag{13}$$

The corresponding boundary conditions are

$$f' = 1,\ \ f = -f_w,\ \ \theta = 1,\ \ \varphi = 1 \qquad \text{at} \qquad \eta = 0$$

$$f'(\infty) \to 0, \quad \theta(\infty) \to 0 \quad \varphi(\infty) \to 0 \ \text{ as } \quad \eta \to \infty \tag{14}$$

where prime denotes differentiation with respect to η. η is the similarity variable, $f(\eta)$ -the dimensionless stream function, $f'(\eta)$ - the dimensionless velocity, $\theta(\eta)$- the dimensionless temperature, $\theta(\eta)$ - the dimensionless concentration f_w - is the non-dimensional suction velocity, *Gr* - the local thermal Grashof number, *Gc* - the modified Grashof number, *M* - the local magnetic field parameter, *K*- the permeability parameter, *R* - the radiation parameter, *Pr* - the Prandtl number, *Du* - the Dufour number, *Sc* - the Schmidt number, *Sr* - the Soret number, *S* - the heat source parameter, *Kr* - the chemical reaction parameter and *Nc* - the concentration difference parameter.

For the type of technical problem under consideration, the main physical quantities of interest are the skin friction coefficient $f''(0)$, local Nusselt number $-\theta'(0)$ and the Sherwood number $-\varphi'(0)$ represent the wall shear stress, the heat and mass transfer rates at the surface respectively. Our task is to investigate how the values of $f''(0)$, $-\theta'(0)$ and $-\varphi'(0)$ vary with the local thermal Grashof number, modified Grashof number, local magnetic field parameter, permeability parameter, radiation parameter, the Prandtl number, Dufour number, Schmidt number, Soret number, heat source parameter, chemical reaction parameter and concentration difference parameter.

3. NUMERICAL SOLUTION OF PROBLEM

The equations governing the flow are coupled non-linear differential equations and solved numerically by using the Newton–Raphson shooting method along with Runge–Kutta fourth order. First of all, writing the set of higher order non-linear differential equations (12), (13) and (14) into simultaneous differential equations of first order as follows.

Let $f = y_1, f' = y_2, f'' = y_3, \theta = y_4, \theta' = y_5, \varphi = y_6, \varphi' = y_7$.

Thus, the corresponding first order differential equations are

$$\frac{dy_1}{d\eta} = y_2, \quad \frac{dy_2}{d\eta} = y_3, \quad \frac{dy_3}{d\eta} = -\{y_1 y_3 - y_2^2 + Gry_4 + Gcy_6 - (M+K)y_2\},$$

$$\frac{dy_4}{d\eta} = y_5, \quad \frac{dy_5}{d\eta} = \frac{-1}{(4R+1)}\{\Pr(y_1 y_5 - y_2 y_4) + Du\Pr(\frac{dy_7}{d\eta}) + \Pr S y_4\}, \quad \frac{dy_6}{d\eta} = y_7,$$

$$\frac{dy_7}{d\eta} = -\{Sc(y_1 y_7 - y_2 y_6) + SrSc(\frac{dy_5}{d\eta}) - ScKr(y_6 + Nc)\},$$

subject to the following initial conditions

$$y_1(0) = -f_w,\ y_2(0) = 1, \quad y_4(0) = 1,\ y_6(0) = 1,$$

$$y_2(\infty) = 0,\ y_4(\infty) = 0,\ \ y_6(\infty) = 0$$

Then the set of above equations transformed into initial value problem by applying the Newton Raphson shooting technique. A step size of $\Delta\eta = 0.01$ is chosen to satisfy the convergence criterion of 10^{-6} in nearly all cases. From the process of numerical computation, the skin-friction coefficient, Nusselt number and Sherwood number which are respectively proportional to $f''(0)$, $-\theta'(0)$, and $-\varphi'(0)$ are also sorted out and their numerical values are presented in tabular form.

4. RESULTS AND DISCUSSION

In order to get a physical insight into the problem, a parametric study is conducted to illustrate the effects of different governing parameters on the velocity, temperature and concentration upon the nature of flow and transport, and presented graphically in Figs. 2-30. Here the value of *Pr* is chosen as 0.71, which corresponds to air and the value of *Sc* are chosen as 0.62, which corresponds to water vapor and the other parameters are chosen arbitrarily

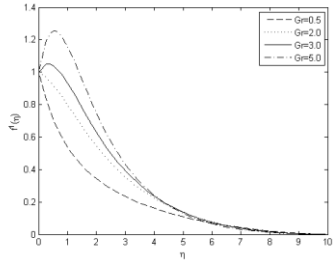

Fig. 2 Velocity profiles for Gr

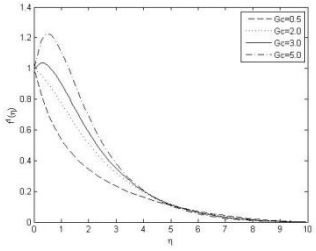

Fig. 3 Velocity profiles for *Gc*

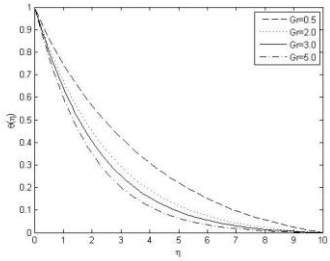

Fig. 4 Temperature profiles for *Gr*

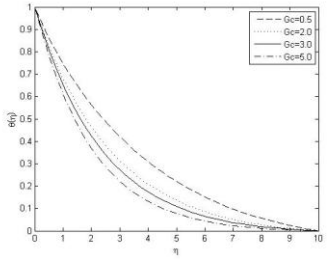

Fig. 5 Temperature profiles for *Gc*

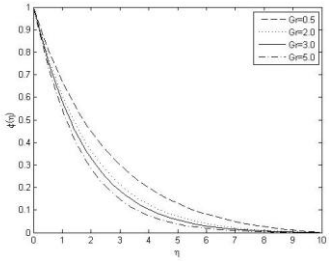

Fig. 6 Concentration profiles for *Gr*

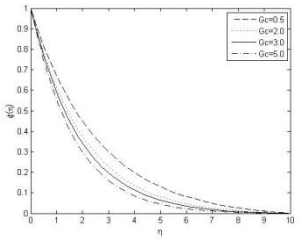

Fig. 7 Concentration profiles for *Gc*

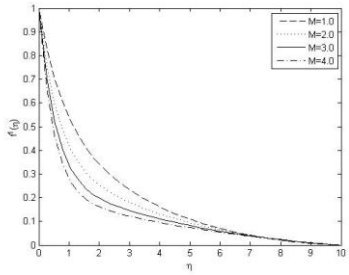

Fig. 8 Velocity profiles for *M*

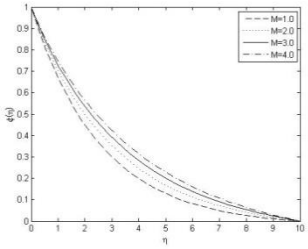

Fig. 9 Temperature profiles for *M*

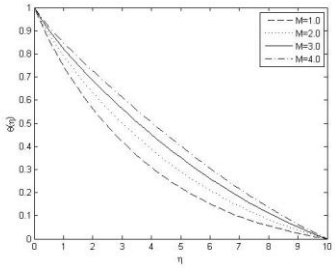

Fig. 10 Concentration profiles for *M*

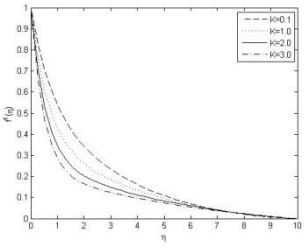

Fig. 11 Velocity profiles for *K*

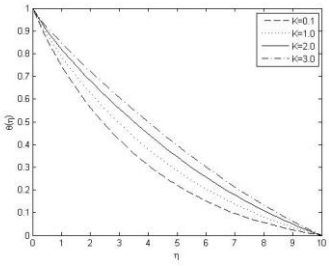

Fig. 12 Temperature profiles for *K*

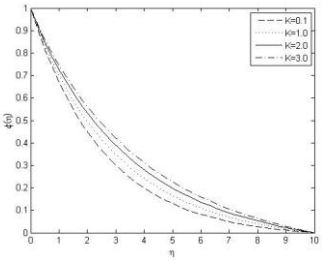

Fig. 13 Concentration profiles for *K*

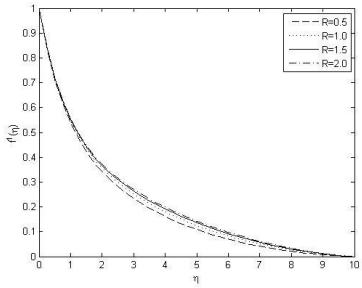

Fig. 14 Velocity profiles for *R*

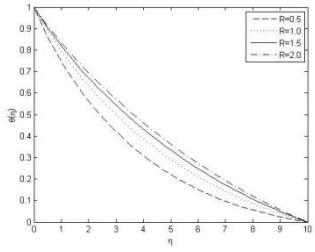

Fig. 15 Temperature profiles for *R*

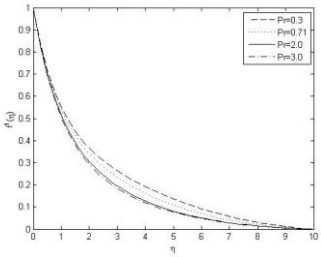

Fig. 16 Velocity profiles for *Pr*

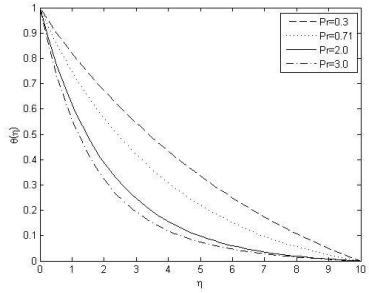

Fig. 17 Temperature profiles for *Pr*

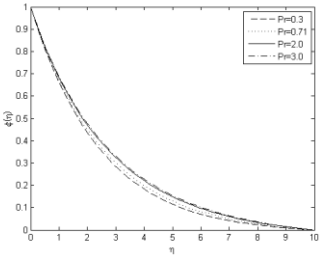

Fig. 18 Concentration profiles for *Pr*

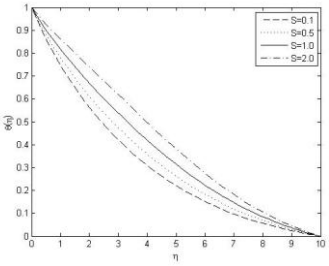

Fig. 19 Temperature profiles for *S*

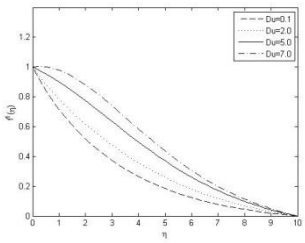

Fig. 20 Velocity profiles for *Du*

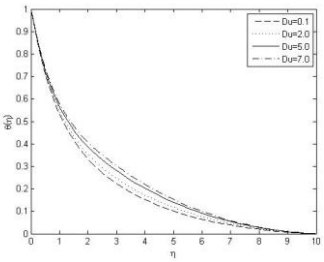

Fig. 21 Temperature profiles for *Du*

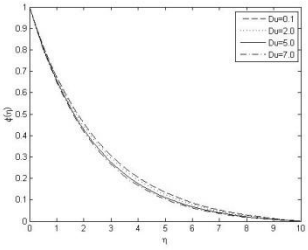

Fig. 22 Concentration profiles for *Du*

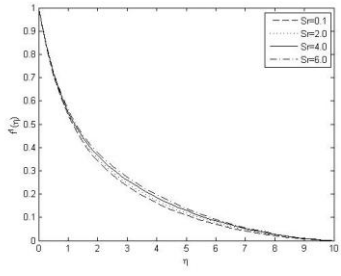

Fig. 23 Velocity profiles for *Sr*

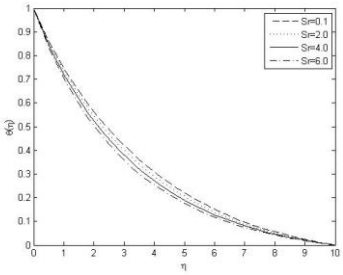

Fig. 24 Temperature profiles for *Sr*

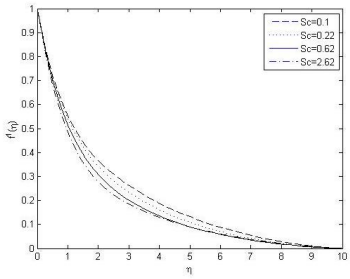

Fig. 25 Velocity profiles for *Sc*

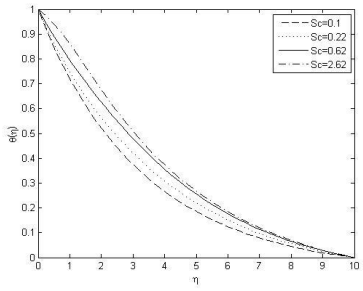

Fig. 26 Temperature profiles for *Sc*

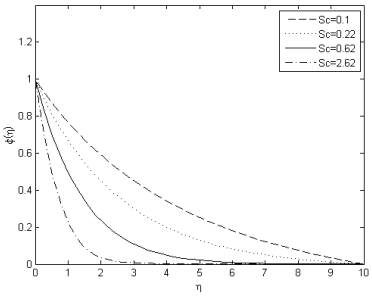

Fig. 27 Concentration profiles for *Sc*

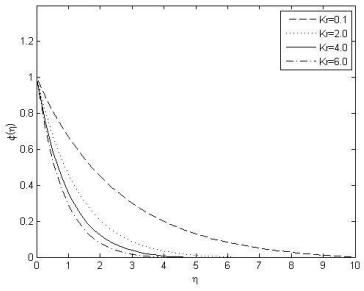

Fig. 28 Concentration profiles for *Kr*

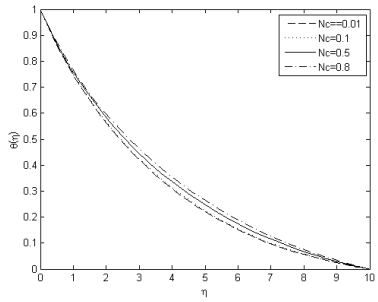

Fig. 29 Temperature profiles for *Nc*

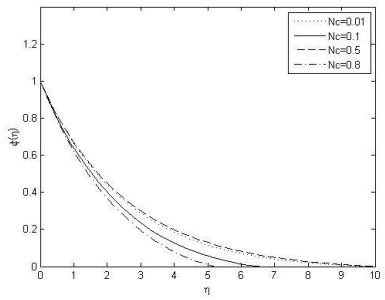

Fig. 30 Concentration profiles for *Nc*

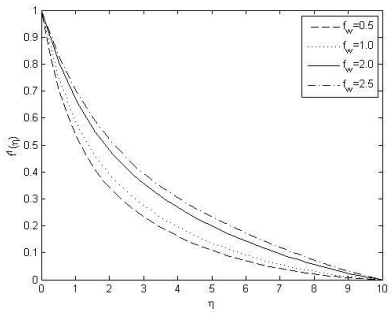

Fig. 31 Velocity profiles for *fw*

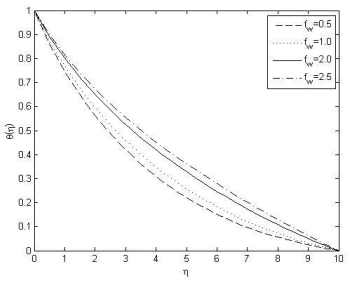

Fig. 32 Temperature profiles for *fw*

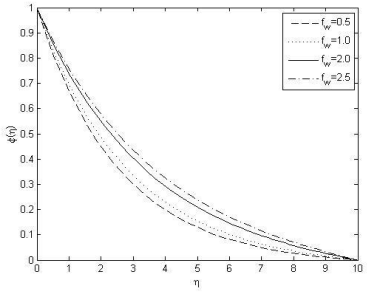

Fig. 33 Concentration profiles for *fw*

Table 1: Comparison of $f''(0)$, $-\theta'(0)$, $-\varphi'(0)$ when $Gr=Gc=0.1$, $Du=0.1$, $Sr=1.0$, $f_w=0.1$ for different values of M, K and Pr

M	K	Pr	*Srinivasa Rao et al*			*Present results*		
			$-f''(0)$	$-\theta'(0)$	$-\varphi'(0)$	$-f''(0)$	$-\theta'(0)$	$-\varphi'(0)$
0.1	0.1	0.72	0.915677	0.793711	0.260249	1.915675	0.793713	0.260249
0.5	0.1	0.72	1.09468	0.753282	0.242587	1.094677	0.753279	0.242588
0.1	1.0	0.72	1.28898	0.710393	0.226773	1.288978	0.710392	0.226774
0.1	0.1	1.0	0.920067	0.965159	0.224252	0.920067	0.965159	0.224253

Table 2: Comparison of $f''(0)$, $-\theta'(0)$, $-\varphi'(0)$ when

$Gr=Gc=0.1$, $M=0.1$, $K=0.1$, $Pr=0.72$, Sr=1.0 for different values of Du, Sc and f_w

Du	*Sc*	f_w	*Srinivasa Rao et al*			*Present results*		
			$-f''(0)$	$-\theta'(0)$	$-\varphi'(0)$	$-f''(0)$	$-\theta'(0)$	$-\varphi'(0)$
1.0	0.22	0.1	0.912726	0.73387	0.273729	0.912725	0.733871	0.273729
0.1	0.62	0.1	0.925313	0.771746	0.422095	0.925471	0.778447	0.418680
0.1	0.22	0.5	0.758705	0.672326	0.263817	0.758703	0.672322	0.263820

Table 1 and Table 2 presents a comparison of $f''(0)$, $-\theta'(0)$ and $-\varphi'(0)$ between the present results and the results obtained by Srinivasa Rao *et al.* [33] for the reduced case $R=S=Kr=Nc=0$ and found that there is a good agreement.

Table 3: Numerical values of the skin friction $f''(0)$, Nusselt number $-\theta'(0)$ and the Sherwood number $-\varphi'(0)$ for $R=0.5$, $Pr=0.71$, $S=0.1$, $Du=1.0$, $Sr=0.1$, $Sc=0.22$, $Kr=0.1$ and $Nc=0.01$

Gr	*Gc*	*M*	*K*	f_w	$f''(0)$	$-\theta'(0)$	$-\varphi'(0)$
0.5	0.5	1.0	0.1	0.5	−0.725034	0.303159	0.408861
2.0	0.5	1.0	0.1	0.5	−0.071571	0.387802	0.480307
3.0	0.5	1.0	0.1	0.5	0.329528	0.423252	0.512401
5.0	0.5	1.0	0.1	0.5	1.082561	0.475534	0.561335
0.5	0.5	1.0	0.1	0.5	−0.725034	0.303159	0.408861
0.5	2.0	1.0	0.1	0.5	−0.096652	0.377842	0.472762
0.5	3.0	1.0	0.1	0.5	0.293020	0.411553	0.503195
0.5	5.0	1.0	0.1	0.5	1.027620	0.462321	0.550455
0.5	0.5	1.0	0.1	0.5	−0.725034	0.303159	0.408861
0.5	0.5	2.0	0.1	0.5	−1.084967	0.255532	0.370205
0.5	0.5	3.0	0.1	0.5	−1.386501	0.219656	0.341598
0.5	0.5	4.0	0.1	0.5	−1.649319	0.191944	0.319700
0.5	0.5	1.0	0.1	0.5	−0.725034	0.303159	0.408861
0.5	0.5	1.0	1.0	0.5	−1.052040	0.259697	0.373551
0.5	0.5	1.0	2.0	0.5	−1.358326	0.222827	0.344113
0.5	0.5	1.0	3.0	0.5	−1.624421	0.194425	0.321655
0.5	0.5	1.0	0.1	0.5	−0.725034	0.303159	0.408861
0.5	0.5	1.0	0.1	1.0	−0.600602	0.257632	0.370567
0.5	0.5	1.0	0.1	2.0	−0.428277	0.231095	0.306210
0.5	0.5	1.0	0.1	2.5	−0.369269	0.212796	0.279407

Table 4: Numerical values of the skin friction $f''(0)$, Nusselt number $-\theta'(0)$ and the Sherwood number $-\varphi'(0)$ for $Gr=Gc=0.5$, $M=1.0$, $K=0.1$, $Sr=0.1$, $Sc=0.22$, $Kr=0.1$ and $Nc=0.01$

R	*S*	*Pr*	*Du*	$f''(0)$	$-\theta'(0)$	$-\varphi'(0)$
0.5	0.1	0.71	1.0	−0.725034	0.303159	0.408861
1.5	0.1	0.71	1.0	−0.716828	0.237456	0.414328
1.5	0.1	0.71	1.0	−0.712548	0.204416	0.417203
2.0	0.1	0.71	1.0	−0.709898	0.184348	0.418986
0.5	0.1	0.71	1.0	−0.725034	0.303159	0.408861
0.5	0.1	0.71	1.0	−0.719597	0.262643	0.412347
0.5	0.2	0.71	1.0	−0.713188	0.216581	0.416423
0.5	0.3	0.71	1.0	−0.705527	0.163364	0.421209

0.5	0.4	0.3	1.0	−0.712387	0.203184	0.417311
0.5	0.1	0.71	1.0	−0.725034	0.303159	0.408861
0.5	0.1	2.0	1.0	−0.747303	0.500829	0.394875
0.5	0.1	3.0	1.0	−0.757193	0.601008	0.389290
0.5	0.1	0.71	0.1	−0.730770	0.351073	0.405242
0.5	0.1	0.71	2.0	−0.718623	0.249458	0.412779
0.5	0.1	0.71	5.0	−0.699198	0.085445	0.423953
0.5	0.1	0.71	7.0	−0.686107	0.026337	0.430994

Table 5: Numerical values of the skin friction $f''(0)$, Nusselt number $-\theta'(0)$ and the Sherwood number $-\varphi'(0)$ for Gr=Gc=0.5, M=1.0, K=0.1, R=0.5, Pr=0.71, S=0.1 and Du=1.0

Sc	Sr	Kr	Nc	$f''(0)$	$-\theta'(0)$	$-\varphi'(0)$
0.1	0.1	0.1	0.01	−0.711758	0.339232	0.271937
0.22	0.1	0.1	0.01	−0.725034	0.303159	0.408861
062	0.1	0.1	0.01	−0.74855	0.232978	0.689894
2.62	0.1	0.1	0.01	−0.785018	0.096587	1.276235
0.22	0.1	0.1	0.01	−0.725034	0.303159	0.408865
0.22	2.0	0.1	0.01	−0.719224	0.319705	0.346172
0.22	4.0	0.1	0.01	−0.712116	0.339256	0.269175
0.22	6.0	0.1	0.01	−0.703831	0.361517	0.178016
0.22	0.1	0.1	0.01	−0.725034	0.303159	0.408861
0.22	0.1	2.0	0.01	−0.753518	0.213953	0.769920
0.22	0.1	4.0	0.01	−0.767888	0.156309	1.015446
0.22	0.1	6.0	0.01	−0.777462	0.110697	1.212027
0.22	0.1	0.1	0.01	−0.725034	0.303159	0.408861
0.22	0.1	0.1	0.1	−0.725732	0.301155	0.414792
0.22	0.1	0.1	0.5	−0.728843	0.291902	0.441517
0.22	0.1	0.1	0.8	−0.731187	0.284548	0.461979

5. CONCLUSIONS

- An increase in the buoyancy parameters (Gc or Gr) enhances the velocity, skin friction coefficient, Nusselt number and Sherwood number but reduces the temperature and concentration.
- An increase in the magnetic parameter or permeability parameter, leads to an increase in the temperature and concentration and a decrease in the velocity, skin-friction coefficient, Nusselt number and Sherwood number.
- There is an increase in the velocity, temperature and concentration while the skin-friction coefficient, Nusselt number and Sherwood number decrease with an increase in the suction parameter.
- As the radiation parameter or the heat source parameter increases, there is an increase in the temperature, skin friction coefficient and Sherwood number and a decrease in the Nusselt number. An increase in the radiation parameter also leads to a decrease in the velocity.
- With an increase in the Prandtl number both the concentration and Nusselt number increase, while the velocity, temperature, skin friction coefficient and Sherwood number decrease.
- An increase in the Dufour number leads to an increase in the velocity, temperature, skin friction coefficient and Sherwood number while a decrease in the concentration and Nusselt number.
- An increase in the Soret number increases the velocity, skin friction coefficient and Nusselt number while decreases the temperature and Sherwood number.

- The concentration, skin friction coefficient and Nusselt number decrease while the Sherwood number increases with an increase in the Schmidt number or chemical reaction parameter or concentration difference parameter. An increase in the Schmidt number also leads to increase in the velocity.
- An increase in the suction parameter enhances the velocity, temperature, concentration and skin friction co-efficient but reduces the Nusselt number and Sherwood number.

REFERENCES

1. V.M. Soundalgekar, Convection Effects on the Stokes Problem for Infinite Vertical Plate, ASME. J. Heat Transfer, 99 (1997) 499-501.
2. V.M. Soundalgekar, Effects of Mass Transfer and Free Convection on the Flow Past an Impulsively Started Vertical Flat Plate, ASME Jounal Appl. Mech., 46 (1979) 757-760.
3. A.Bejan, K.R.Khair, Heat and mass transfer by natural convection in a porous medium, Int. J. Heat Mass Transfer, 28 (1985) 909-918.
4. R.Cortell, Suction, viscous dissipation and thermal radiation effects on the flow and heat transfer of a power-law fluid past an infinite porous plate, Chem Eng Res Des, (2010), doi:10.1016/j.cherd.2010.04.017
5. N.G.Kafoussias, E.W.Williams, Thermal-diffusion and diffusion-thermo effects on mixed free-forced convective and mass transfer boundary layer flow with temperature dependent viscosity. International Journal of Engineering Science, 33(9) (1995) 1369-1384.
6. F.S.Ibrahim A.M.Elaiw, A.A.Bakr, Effect of chemical reaction and radiation absorption on unsteady MHD free convection flow past a semiinfinite vertical permeable moving plate with heat source/suction. Communication in Non-Linear Science and Numerical Simulation, 13(6) (2008) 1056-1066.
7. S.Y.Ibrahim, O.D.Makinde, Chemically reacting MHD boundary layer flow of heat and mass transfer over a moving vertical plate with suction, Scientific Research and Essays, 19 (2010) 2875-2882.
8. G.Srinivasa Rao, B.Ramana, B.Rami Reddy, G.Vidyasagar, Soret and Dufour effects on MHD Boundary layer flow over a Moving Vertical porous plate with suction International Journal of Emerging Trends in Engineering and Development, 2(4) (2014) 2249-6149.

9.M.Q.Brewster, Thermal radiative transfer and properties, (1992) John Wiley & Sons, NewYork.